PHYSICAL REVIEW B VOLUME 14, NUMBER 1 1 JULY 1976

Dynamics of a system of randomly distributed spins with multipolar interactions: Application to dipolar systems

Charles W. Myles*
Battelle Memorial Institute, 505 King Avenue, Columbus, Ohio 43201

C. Ebner
Department of Physics, The Ohio State University, Columbus, Ohio 43210
and Battelle Memorial Institute, 505 King Avenue, Columbus, Ohio 43201

Peter A. Fedders†
Arthur Holly Compton Laboratory of Physics, Washington University, St. Louis, Missouri 63130
(Received 4 August 1975)

A general first-principles method for the calculation of dynamical spin correlation functions in a system of randomly distributed, strongly interacting spins with multipolar interactions is presented. The method is valid in the high-temperature limit and is applicable at all spin concentrations c. As a numerical example, the case of dipolar forces is treated and the magnetic-resonance frequency line shape is calculated for a variety of values of c. The general trend of the change in line shape with c obtained agrees with phenomenological theories and with experiment. The theoretical linewidth has the correct c dependence in both the $c \to 1$ and $c \to 0$ limits.

I. INTRODUCTION

There have been a number of calculations of the spectral functions for a system of randomly distributed impurity spins with pairwise interactions proportional to r^{-n}, where r is the distance separating a pair.[1-11] Many of these treatments are semiphenomenological in that they assume a functional form for a spin correlation function which is then averaged over some assumed distribution.[1-8] Also, many of them refer exclusively to either the high-[1-3,7] or the low-concentration[3-7,9-11] limit. In this paper we present a first-principles method of calculation, applicable at *all* concentrations and valid in the high-temperature limit, which is based on a rigorously formulated theory of interacting spins that has previously been used successfully to calculate spectral functions for perfect lattices of spins.[12-15] We have previously presented a brief summary of this theory[16] along with some preliminary results. It is the purpose of this paper to present a detailed discussion of the general theory along with some numerical results for the special case of dipolar forces.

Although radically different and sometimes contradictory assumptions are made by different investigators, most of them obtain theoretical linewidths which have the experimentally observed dependence on the spin concentration c in both the small- ($c \to 0$) and the large- ($c \to 1$) concentration limits. The reason for this is that almost any set of reasonable assumptions should give the correct concentration dependence in the limiting cases. For example, as $c \to 1$, one expects the linewidth to be scaled as the square root of the average of the second moment M_2. Since the average of M_2 is proportional to c independent of the interaction,[2,3] the linewdith should be proportional to $c^{1/2}$.[2,3,7,8,12] On the other hand, as $c \to 0$ one would expect the linewidth to be proportional to r_0^{-n}, where r_0 is an average interspin spacing.[3] Thus, since $r_0 \propto c^{-1/3}$, one expects the linewidth to be proportional to $c^{n/3}$.[3-11]

An example is the calculation in Ref. 8, where it is assumed that each spin decays via a Gaussian process which is scaled by the second moment it sees. The total spectral function is obtained by averaging this function over an appropriate distribution. This method yields the correct concentration dependence in the limiting cases and is an excellent method to use with a moment fit. However, there is no reason to believe that all of the spins really decay via Gaussian processes. In fact, even if $c = 1$, the process is not Gaussian, since NMR spectra of dipolar systems show an oscillatory long-time behavior.[17] Other investigators, on the other hand, obtain a spectral function for low concentrations by averaging over the exact spectral functions of individual pairs.[7] Although this procedure also yields reasonable results, the assumption taken literally means that the system consists of an ensemble of pairs that do not interact with each other. Thus there can be no true spin decay, since each pair can last forever in an excited eigenstate. In other theories the physical nature of the approximation is rather unclear and/or cannot be improved upon.

One such theory is that of Sung and Arnold[9]; these authors present a method for calculating spectral functions self-consistently as functions of c. Although their formalism produces results which are in agreement with experiment in several cases,[9-11] we believe that the approximations made in the derivation of their basic equations for the average correlation functions are rather obscure physically and do not easily lend themselves to improvement. Furthermore, they calculate only an autocorrelation function which, in the case of NMR and EPR experiments, is *not* the physically observed function. Rather, the observed function is the $\vec{q}=0$ limit of a function like $\langle S_+(\vec{q},t)S_-(\vec{q},0)\rangle$, where $S_\pm(\vec{q})$ are the Fourier-transformed spin-raising and -lowering operators and the brackets $\langle\cdots\rangle$ denote a thermal average. For example, for dipolar forces the Fourier transform of the correlation function

$$\lim_{\vec{q}\to 0}\langle S_z(\vec{q},t)S_z(\vec{q},0)\rangle$$

should be a δ function in frequency space no matter what the distribution of spins. This can be clearly seen if one takes moments of this function in the presence of the truncated dipolar interaction. On the other hand, in the course of the investigation presented in this paper we calculated the averaged correlation functions for the case of the truncated dipolar interaction via the Sung-Arnold method and found that the zz correlation function is not a δ function. Although our own approximations are certainly not unassailable, we believe that they are physically well motivated and are capable of being extended.

The remainder of this paper is organized as follows: In Sec. II we derive the first-principles method of calculating the spectral functions for a random distribution of spins whose pairwise interactions have an r-dependence of the form r^{-n}. In particular, nonlinear integral equations are obtained for the average spectral functions. Section III contains the solutions to these equations for several spin concentrations in the case of a dipolar ($n=3$) spin-spin interaction, and in Sec. IV may be found a critique of our method and a summary. The Appendix presents a discussion of the probability distribution function used in the calculations of Sec. III.

II. METHOD

The method employed in our calculation is a variation of a diagrammatic technique we have used in other spin problems.[12-15] It has been successful in treating systems of perfect lattices of interacting spins and involves no line-shape assumptions or adjustable parameters. Following Ref. 12 we define a set of diagonal two-point correlation functions as

$$G_\alpha(i,j;t)=\langle A_\alpha(i,t)A_\alpha^\dagger(j,0)\rangle\Theta(t), \tag{1}$$

where $\Theta(t)$ is the step function, the angular brackets denote the average in the canonical ensemble, and italic letters denote lattice sites containing spins. The irreducible multipole operators $A_\alpha(i)$, where $\alpha=(l_\alpha,m_\alpha)$, for $l\leq 2s$, form a complete set of spin operators at the site i. These operators and their relationship to the usual vector spin operators are discussed elsewhere.[12,18] One of our basic assumptions is that either the Zeeman energy or the isotropic part of the spin-spin interaction is much greater than the anisotropic part of the interaction. Although this restriction is not necessary, it is convenient, since it allows us to neglect the off-diagonal Green's functions.

In this paper we consider the spin Hamiltonian

$$H=\hbar\omega_0\sum_i S_z(i)+\frac{1}{2}\sum_{i,j,\alpha,\beta}A_\alpha(i)J_{\alpha\beta}(i,j)A_\beta(j), \tag{2}$$

where $\omega_0=\gamma H_0$, γ is the gyromagnetic ratio, and $\vec{H}_0$ is an external magnetic field whose direction defines the z axis. Dipole-dipole, quadrupole-quadrupole, or other types of spin-spin interactions can be described by this general Hamiltonian when the potential $J_{\alpha\beta}(i,j)$ (multipolar in nature) is specified. In this and all subsequent equations, only occupied lattice sites are summed over.

We will work in the high-temperature limit, where all spin energies are much smaller than kT. In this temperature regime it is convenient to express the Green's function in terms of a mass operator or self-energy $\Sigma_\alpha(i,j;t)$ defined by the equation[12]

$$\left(i\frac{\partial}{\partial t}-m_\alpha\omega_0\right)G_\alpha(i,j;t)-\sum_k\int d\bar{t}\,\Sigma_\alpha(i,k;t-\bar{t})G_\alpha(k,j;\bar{t})=i\delta_{i,j}\delta(t). \tag{3}$$

In earlier work[12-15] we have used the "bubble approximation" for the self-energy. A straightforward application of this approximation at $T=\infty$ with the Hamiltonian given by Eq. (2) yields

$$\Sigma_\alpha(i,i';t)=i\sum_{\beta,\gamma,j,j'}\Omega_{\alpha\beta\gamma}(i,j)[\Omega^*_{\alpha\beta\gamma}(i',j')G_\beta(i,i';t)G_\gamma(j,j';t)+\Omega^*_{\alpha\gamma\beta}(i',j')G_\beta(i,j';t)G_\gamma(j,i',t)], \tag{4}$$

where

$$\Omega_{\alpha\beta\gamma}(i,j) = \sum_{\delta} \frac{c(\alpha;\delta;\beta)J_{\delta\gamma}(i,j)}{\hbar} \tag{5a}$$

and

$$[A_\alpha, A_\beta] = \sum_{\gamma} c(\alpha;\beta;\gamma)A_\gamma. \tag{5b}$$

The justification for the use of the bubble approximation in this problem is that it is the lowest-order approximation in a well-defined hierachy of self-consistent approximations and that it has yielded results in good agreement with experiment when applied to a variety of other spin problems.[12-15] Since it is our contention that the spectral line shape at all concentrations is dominated by interactions of a given spin with a group of other spins, and not by a single other spin, there is no *a priori* reason why the bubble approximation should be worse for the dilute spin system than for the dense spin system. We shall use these concepts below, and discuss the validity of our approximations further at the end of this section.

Even though Eqs. (3) and (4) are nonlinear integral equations in four variables,[12] they can, in principle, be solved by computer for the case of a perfect lattice. For a random distribution of impurities, however, this is not a feasible approach. As a first step toward the simplification of these equations, while still retaining their basic physics, we define, as in Ref. 12, a local correlation function $G_\alpha(i,t)$ and local self-energy $\Sigma_\alpha(i,t)$ which satisfy Eqs. (3) and (4) if G_α is entirely local, so that $G_\alpha(i,j;t) = G_\alpha(i,t)\delta_{ij}$:

$$\left(i\frac{\partial}{\partial t} - m_\alpha\omega_0\right)G_\alpha(i,t) - \int d\bar{t}\ \Sigma_\alpha(i,\bar{t})G_\alpha(i,t-\bar{t}) = i\delta(t), \tag{6}$$

$$\Sigma_\alpha(i,t) = i\sum_{j,\beta,\gamma} |\Omega_{\alpha\beta\gamma}(i,j)|^2 G_\beta(i,t)G_\gamma(j,t). \tag{7}$$

It is shown in Ref. 12 that this local approximation introduces errors in the solution for the correlation functions which are of the order of $1/Z$, where Z is the number of spins in the interaction range of a given spin. Since the bubble approximation is itself in error by numbers of the same order, this additional approximation should not affect the validity of the theory.

We next approximate the solution to Eqs. (3) and (4) by substituting $G_\alpha(i,j;t) = \delta_{ij}G_\alpha(i,t)$ with $G_\alpha(i,t)$ obtained from Eqs. (6) and (7), into Eq. (4). This will yield a good "nonlocal" correlation function under the conditions just discussed. Note that $G_\alpha(i,t)$ is itself not a good solution to Eqs. (3) and (4), but it can be used to generate a good solution.

For a perfect lattice, $G_\alpha(i,t)$ does not depend on the lattice site i. However, for a distribution of impurity spins, the local function $G_\alpha(i,t)$ depends on its immediate environment. In order to solve Eqs. (6) and (7) for this case we make the ansatz that it is reasonable to replace $G_\gamma(j,t)$ in Eq. (7) by the average local Green's function $\bar{G}_\gamma(t)$,

$$\bar{G}_\gamma(t) = N^{-1}\sum_i G_\gamma(i,t), \tag{8}$$

where N is the number of impurity spins. This is an effective-medium approximation (EMA), reminiscent of the coherent-potential approximation[19] (CPA). Physically, one can interpret Eq. (7) as saying that the spin dynamics at site i depend on the other spins through their positions and through their fluctuation spectra $G_\gamma(j,t)$. The EMA replaces Eq. (7) by

$$\Sigma_\alpha(i,t) = i\sum_{j,\beta,\gamma} |\Omega_{\alpha\beta\gamma}(i,j)|^2 G_\beta(i,t)\bar{G}_\gamma(t), \tag{7'}$$

which in effect says that the spin dynamics at site i depend on the other spins through their positions and through an *average* fluctuation spectrum. In other words, we are replacing the fluctuation spectrum seen by a spin at site i by an average or effective fluctuation spectrum. Hence the terminology "effective-medium approximation."

With this additional approximation Eqs. (6), (7'), and (8) can be solved self-consistently to obtain $G_\alpha(i,t)$ and $\bar{G}_\alpha(t)$. Using the local approximation for the G's and the EMA in Eq. (4) for $\Sigma_\alpha(i,j;t)$, we find that it becomes

$$\Sigma_\alpha(i,j;t) = i\sum_{\beta,\gamma,k} |\Omega_{\alpha\beta\gamma}(i,k)|^2 G_\beta(i,t)\bar{G}_\gamma(t)\delta_{ij} + i\sum_{\beta,\gamma} \Omega_{\alpha\beta\gamma}(i,j)\Omega^*_{\alpha\gamma\beta}(j,i)G_\beta(i,t)\bar{G}_\gamma(t). \tag{9}$$

Perhaps it is worthwhile at this point to mention the reasons why the CPA and other related techniques are probably not applicable to the problem under consideration. There are basically two reasons for this. First of all, the CPA is usually used to calculate fluctuations about a mean field as a function of concentration. In the present case, however, the mean field is zero, since we are in the $T\to\infty$ limit. Thus there are no well-defined elementary excitations in the problem

and the usual CPA methods appear to break down in this case. Second, the CPA as usually applied treats systems with short-range forces and site diagonal disorder. On the other hand, in the present case, the forces are longer ranged ($\sim r^{-n}$) and thus the system displays off-diagonal disorder. Thus it appears that the system we are considering is in a totally different regime physically from systems to which the CPA can be easily applied.

Ultimately, since almost all experiments are done at zero wave vector, NMR or EPR experiments measure the spatial average $\bar{F}_\alpha(t)$ of $F_\alpha(i,t)$, where

$$F_\alpha(i,t)=\sum_j G_\alpha(i,j;t). \tag{10}$$

By summing Eq. (3) over j, combining that result with Eq. (9), and using the EMA once more, we obtain

$$\left(i\frac{\partial}{\partial t}-m_\alpha\omega_0\right)F_\alpha(i,t)-i\int d\bar{t}\sum_{j,\beta,\gamma}\left[|\Omega_{\alpha\beta\gamma}(i,j)|^2G_\beta(i;t-\bar{t})\bar{G}_\gamma(t-\bar{t})F_\alpha(i,\bar{t})\right.$$
$$\left.+\Omega_{\alpha\beta\gamma}(i,j)\Omega^*_{\alpha\gamma\beta}(j,i)G_\beta(i;t-\bar{t})\bar{G}_\gamma(t-\bar{t})\bar{F}_\alpha(t)\right]=i\delta(t), \tag{11}$$

where

$$\bar{F}_\alpha(t)=N^{-1}\sum_i F_\alpha(i,t), \tag{12}$$

and $\bar{F}_\alpha(t)$ is the physical function measured and hence the function desired.

The basic equations of our theory, Eqs. (6), (7′), (8), and (10)–(12), can be expressed in terms of a probability distribution function which describes the distribution of the interaction strengths squared. For simplicity suppose that $|\Omega_{\alpha\beta\gamma}(i,j)|^2$ and $\Omega_{\alpha\beta\gamma}(i,j)\Omega^*_{\alpha\gamma\beta}(j,i)$ have the same dependence on i and j, say $g(i,j)$. This is true for dipolar forces. [In those cases for which it is not true, the following analysis can still be made, with the added complication of having to consider several functions $g_l(i,j)$, and consequently needing a probability distribution of several variables rather than of only one.] Given just one $g(i,j)$ we may write

$$\sum_j|\Omega_{\alpha\beta\gamma}(i,j)|^2=B_{\alpha\beta\gamma}f(i),$$
$$\sum_j\Omega_{\alpha\beta\gamma}(i,j)\Omega^*_{\alpha\gamma\beta}(j,i)=B'_{\alpha\beta\gamma}f(i), \tag{13}$$
$$\sum_j g(i,j)=f(i).$$

Now let $p(f;c)\,df$ be the normalized probability that $f=f(i)$ lies between f and $f+df$. After changing variables from i to f, the local equations (6), (7′), and (8) are replaced by

$$\left(i\frac{\partial}{\partial t}-m_\alpha\omega_0\right)G_\alpha(f,t)-i\int d\bar{t}\sum_{\beta\gamma}B_{\alpha\beta\gamma}fG_\beta(f,\bar{t})\bar{G}_\gamma(\bar{t})G_\alpha(f,t-\bar{t})=i\delta(t) \tag{14}$$

and

$$\bar{G}_\gamma(t)=\int_0^\infty p(f;c)G_\gamma(f,t)\,df. \tag{15}$$

These may be solved for the local correlation function $G_\alpha(f,t)$ and the average local function $G_\alpha(t)$. Similarly, the nonlocal equations (11) and (12) now read

$$\left(i\frac{\partial}{\partial t}-m_\alpha\omega_0\right)F_\alpha(f,t)-i\int d\bar{t}\sum_{\beta\gamma}\left[B_{\alpha\beta\gamma}fG_\beta(f,t-\bar{t})\bar{G}_\gamma(t-\bar{t})F_\alpha(f,\bar{t})+B'_{\alpha\beta\gamma}fG_\beta(f,t-\bar{t})\bar{G}_\gamma(t-\bar{t})\bar{F}_\alpha(\bar{t})\right]=i\delta(t) \tag{16}$$

and

$$\bar{F}_\alpha(t)=\int_0^\infty F_\alpha(f,t)p(f;c)\,df. \tag{17}$$

Once $p(f;c)$ is specified, the local equations (14) and (15) can be solved self-consistently for $G_\alpha(f,t)$ and $\bar{G}_\alpha(t)$. The solutions can then be substituted into Eqs. (16) and (17) to determine $\bar{F}_\alpha(t)$.

In the derivation of Eqs. (14)–(17) we have made two types of approximations in addition to the bubble approximation. Both of these approximations work best when each spin has a large number of other spins in the range of its interactions. As $c\to1$, these are clearly good approximations. As $c\to0$, the situation is not as clear. However, if one thinks of a "superlattice" with spin spacings increased to give the correct c, then the approximations are independent of c. Of course, this picture ignores clustering effects. We note in

this regard, however, that if one spin's environment is dominated by one very near neighbor, then the spectral weight of these two spins is pushed into the wings of the distribution. Thus the approximations are best for those spins which contribute to the center of the line, and these are just the spins for which clustering effects can be ignored.

III. SOLUTION FOR DIPOLAR INTERACTION; MAGNETIC-RESONANCE LINE SHAPES

A. Discussion

The theory outlined in Sec. II is applicable to all interactions described by Eq. (2); in this section we solve as an example the dipole-dipole interaction in a simple cubic lattice. Furthermore, since only the central peak of the line shape is relevant for comparison with most magnetic-resonance experiments, we will consider an interaction of the truncated dipolar type.[20] Then the α, β sums in Eq. (2) contain only terms where $\alpha = (1, m)$ and $\beta = (1, m')$. Furthermore, the only correlation functions of interest are those with $\alpha = (1, m)$. Therefore, in what follows, whenever a quantity has Greed indices, those indices will be abbreviated by their m values.

Use of Eqs. (5a) and (5b) for the truncated dipolar interaction yields

$$\Omega_{1,1,0} = -\Omega_{-1,-1,0} = \tfrac{1}{2}\Omega_{1,0,1} = \tfrac{1}{2}\Omega_{0,-1,-1} = -\tfrac{1}{2}\Omega_{0,1,-1} = -\tfrac{1}{2}\Omega_{-1,0,-1} = \frac{1}{\sqrt{3}}\,\frac{s(s+1)}{|\vec{r}_{ij}|^3}\,\hbar\gamma^2(1-3\cos^2\Theta_{ij}), \tag{18}$$

where the (i, j) has been suppressed for the Ω's, all Ω's not shown are zero, and Θ_{ij} is the angle $\vec{r}_{ij}$ makes with the magnetic field direction. The explicit integral equations for this special case can easily be obtained by the use of Eq. (18) in Eqs. (14)–(17). The local and nonlocal equations then become

$$\left(i\frac{\partial}{\partial t} - m\omega_0\right) G_m(f,t) - \int d\bar{t}\,\Sigma_m(f,\bar{t})G_m(f,t-\bar{t}) = i\delta(t), \tag{19}$$

$$\Sigma_1(f,t) = \tfrac{1}{12} i s(s+1)\omega_d^2 f \times [\,4G_1(f,t)\bar{G}_0(t) + G_0(f,t)\bar{G}_1(t)], \tag{20}$$

$$\Sigma_0(f,t) = \tfrac{1}{6} i s(s+1)\omega_d^2 f G_1(f,t)\bar{G}_1(t), \tag{21}$$

$$\bar{G}_m(t) = \int_0^\infty df\, p(f;c)G_m(f,t), \tag{22}$$

$$\left(i\frac{\partial}{\partial t} - m\omega_0\right) F_m(f,t) - \int d\bar{t}\,[\Sigma_m(f,\bar{t})F_m(f,t-\bar{t}) + \hat{\Sigma}_m(f,\bar{t})\bar{F}_m(t-\bar{t})] = i\delta(t), \tag{23}$$

$$\hat{\Sigma}_1(f,t) = \tfrac{1}{6} i s(s+1)\omega_d^2 f \times [\,G_1(f,t)\bar{G}_0(t) + G_0(f,t)\bar{G}_1(t)], \tag{24}$$

$$\hat{\Sigma}_0(f,t) = -\Sigma_0(f,t), \tag{25}$$

and

$$\bar{F}_m(t) = \int_0^\infty df\, p(f;c)F_m(f,t); \tag{26}$$

here s is the spin quantum number, while

$$f \equiv \sum_{\vec{r}_{ij}} (1-3\cos^2\Theta_{ij})^2 \left(\frac{a}{|\vec{r}_{ij}|}\right)^6 \tag{27}$$

and

$$\omega_d \equiv \gamma^2\hbar/a^3. \tag{28}$$

Also, use has been made of the symmetry of the equations in G_1 and G_{-1} to eliminate G_{-1}; hence m is either 0 or 1. The probability distribution function $p(f;c)$ was introduced in Sec. II. The explicit form this function takes for the truncated dipolar interaction and the method we have used to numerically compute it are discussed in the Appendix; $p(f;c)$ for various c is shown in Figs. 1–4, and these figures are discussed in detail in the Appendix.

The procedure we have employed to solve the local and nonlocal equations given above is essentially the same as that which we have used previously[12–15,21] for $c = 1$ systems, except that here we have the added complication of having

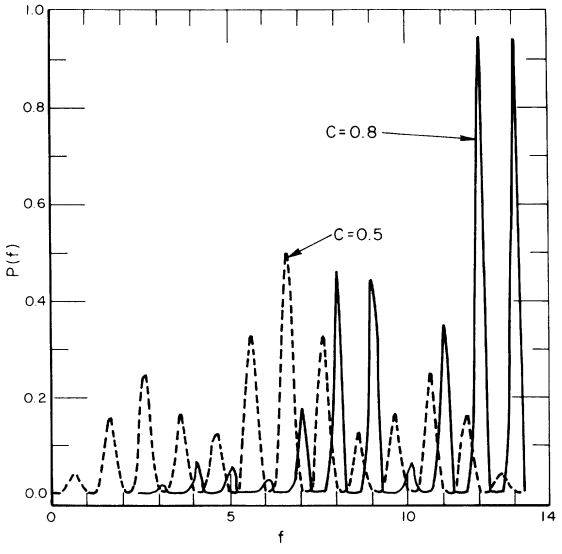

FIG. 1. $p(f;c)$ for $c = 0.8$, 0.5.

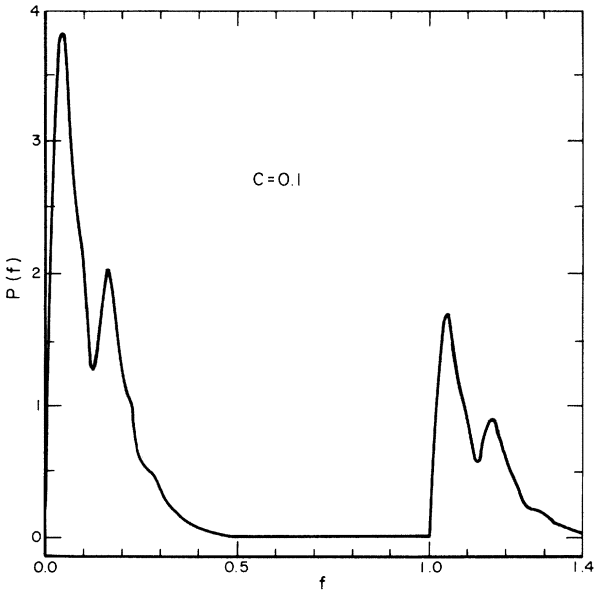

FIG. 2. $p(f;c)$ for $c=0.1$.

to solve integrals over $p(f;c)$. Because of this similarity, for the sake of brevity, only a rough outline of the method is given here.

We begin by defining spectral representations for the frequency-dependent correlation functions and self-energies. These are

$$G_m(f,\omega)=i\int_{-\infty}^{\infty}\frac{d\bar{\omega}}{\pi}\,\frac{g_m(f,\bar{\omega})}{\omega-\bar{\omega}+i\epsilon} \tag{29}$$

and

$$\Sigma_m(f,\omega)=\int_{-\infty}^{\infty}\frac{d\bar{\omega}}{\pi}\,\frac{\Gamma_m(f,\bar{\omega})}{\omega-\bar{\omega}+i\epsilon}$$
$$=\pi_m(f,\omega)-i\Gamma_m(f,\omega); \tag{30}$$

the spectral functions for $\bar{G}_m(\omega)$, $F_m(f,\omega)$, and $\bar{F}_m(\omega)$ are defined similarly to that for $G_m(f,\omega)$ and the spectral function for $\hat{\Sigma}_m(f,\omega)$ is defined

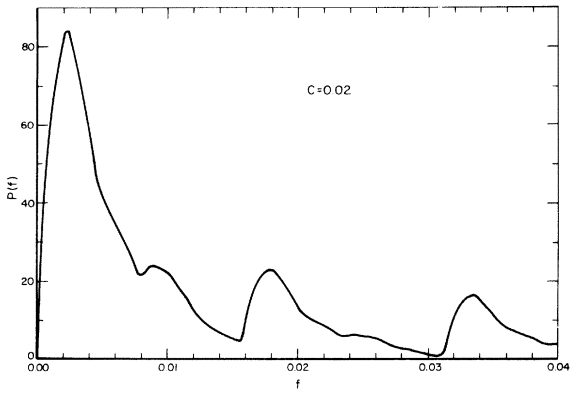

FIG. 3. $p(f;c)$ for $c=0.02$.

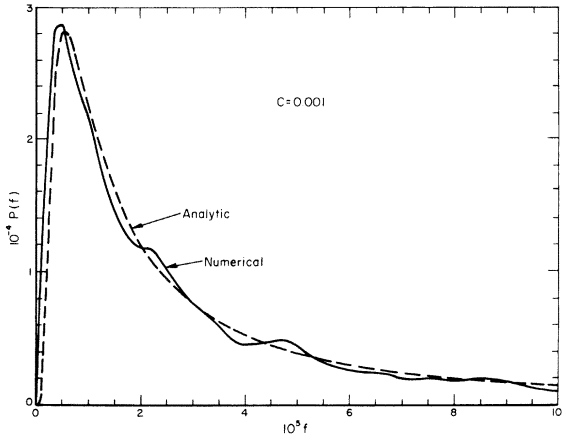

FIG. 4. $p(f;c)$ for $c=0.001$ and the analytic $p(f;c)$ for $c=0.001$ (see the Appendix).

similarly to that for $\Sigma_m(f,\omega)$. After some manipulation it can be shown that the local equations (19)–(22) may be expressed in terms of these spectral functions as

$$g_m(f,\omega)=\frac{\Gamma_m(f,\omega)}{[\omega-\pi_m(f,\omega)]^2+[\Gamma_m(f,\omega)]^2}, \tag{31}$$

$$\Gamma_1(f,\omega)=\frac{s(s+1)}{12}\,\omega_d^2 f \times\int_{-\infty}^{\infty}\frac{d\bar{\omega}}{\pi}\,[4g_1(f,\bar{\omega})\bar{g}_0(\omega-\bar{\omega}) +g_0(f,\bar{\omega})\bar{g}_1(\omega-\bar{\omega})], \tag{32}$$

$$\Gamma_0(f,\omega)=\frac{s(s+1)}{6}\,\omega_d^2 f\int_{-\infty}^{\infty}\frac{d\bar{\omega}}{\pi}\,g_1(f,\bar{\omega})\bar{g}_1(\omega-\bar{\omega}), \tag{33}$$

$$\pi_m(f,\omega)=P\int_{-\infty}^{\infty}\frac{d\bar{\omega}}{\pi}\,\frac{\Gamma_m(f,\bar{\omega})}{\omega-\bar{\omega}}, \tag{34}$$

and

$$\bar{g}_m(\omega)=\int_0^{\infty}df\,p(f;c)g_m(f;\omega). \tag{35}$$

Similarly, the nonlocal equations (23)–(26) can be expressed in terms of spectral functions as

$$\mathfrak{F}_m(\omega)=\frac{\bar{g}_m(\omega)[1+S_m(\omega)]+\bar{h}_m(\omega)T_m(\omega)}{[1+S_m(\omega)]^2+[T_m(\omega)]^2},$$

$$\bar{h}_m(\omega)=P\int_{-\infty}^{\infty}\frac{d\bar{\omega}}{\pi}\,\frac{\bar{g}_m(\bar{\omega})}{\omega-\bar{\omega}}, \tag{36}$$

$$S_m(\omega)=\int_0^{\infty}df\,p(f;c)[g_m(f,\omega)\hat{\Gamma}_m(f,\omega) -h_m(f,\omega)\hat{\pi}_m(f,\omega)], \tag{37}$$

$$T_m(\omega) = \int_0^\infty df\, p(f;c)[g_m(f,\omega)\hat{\pi}_m(f,\omega) + h_m(f,\omega)\hat{\Gamma}_m(f,\omega)], \quad (38)$$

$$\hat{\Gamma}_1(f,\omega) = \frac{s(s+1)}{6}\omega_d^2 f \int_{-\infty}^{\infty} \frac{d\bar{\omega}}{\pi}[g_1(f,\bar{\omega})\bar{g}_0(\omega-\bar{\omega}) + g_0(f,\bar{\omega})\bar{g}_1(\omega-\bar{\omega})], \quad (39)$$

$$\hat{\Gamma}_0(f,\omega) = -\Gamma_0(f,\omega), \quad (40)$$

$$\hat{\pi}_m(f,\omega) = P\int_{-\infty}^{\infty} \frac{d\bar{\omega}}{\pi}\frac{\hat{\Gamma}_m(f,\bar{\omega})}{\omega-\bar{\omega}}, \quad (41)$$

and

$$h_m(f,\omega) = P\int_{-\infty}^{\infty} \frac{d\bar{\omega}}{\pi}\frac{g_m(f,\bar{\omega})}{\omega-\bar{\omega}}, \quad (42)$$

where $\mathfrak{F}_m(\omega)$ is the spectral function for $\bar{F}_m(\omega)$.

The procedure for obtaining solutions is as follows: Choose c and compute $p(f;c)$ (see Appendix); solve the local equations (31)–(35) numerically to self-consistency as outlined in Refs. 12–15 and 21; and substitute these local solutions into the nonlocal equations (36)–(42), and carry out the indicated integrals to obtain the nonlocal average spectral functions $\bar{\mathfrak{F}}_m(\omega)$.

B. Results for $0 \leqslant c \leqslant 1$; experimental comparisons

Since $\hat{\Gamma}_0(f,\omega) = -\Gamma_0(f,\omega)$, it can be seen after a little algebra that

$$\bar{\mathfrak{F}}_0(\omega) = \pi\delta(\omega) \quad (43)$$

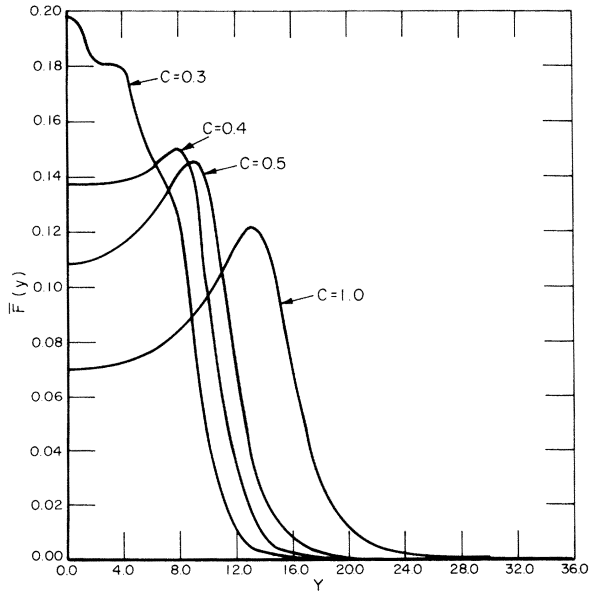

FIG. 5. Average nonlocal function $\bar{F}(y)$ (frequency line-shape function) for $c = 1.0,\ 0.5,\ 0.4,\ 0.3$.

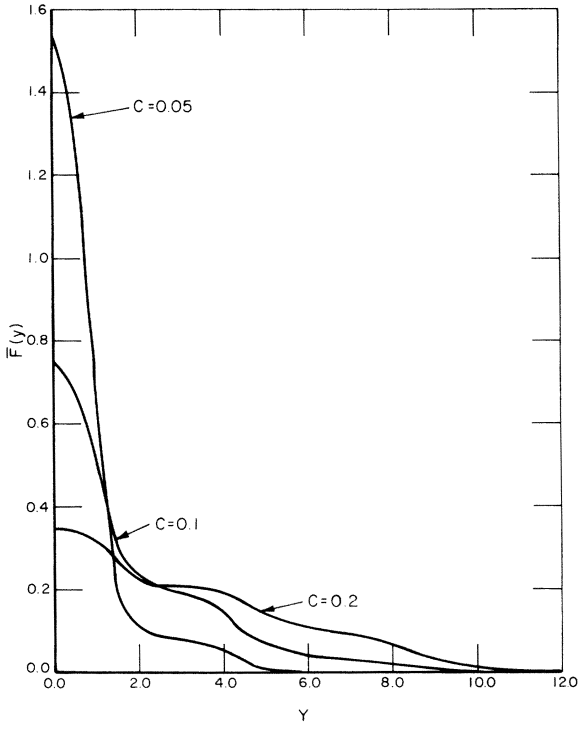

FIG. 6. $\bar{F}(y)$ for $c = 0.2,\ 0.1,\ 0.05$.

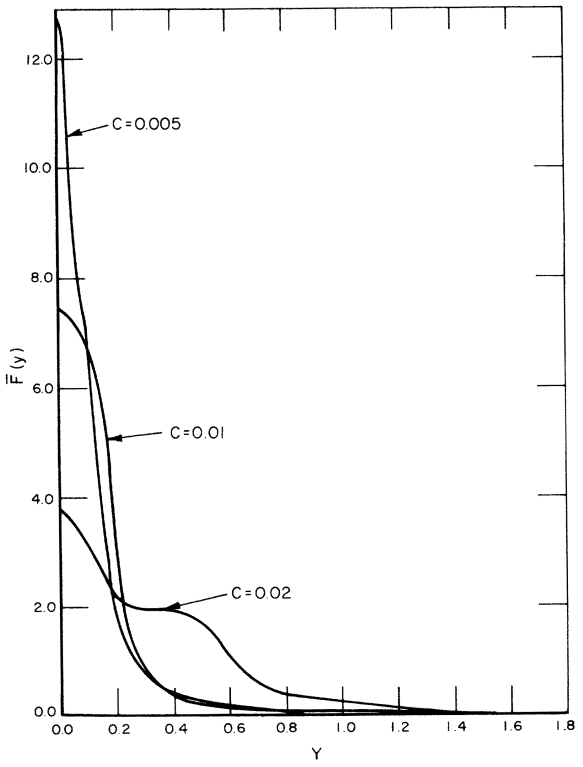

FIG. 7. $\bar{F}(y)$ for $c = 0.02,\ 0.01,\ 0.005$.

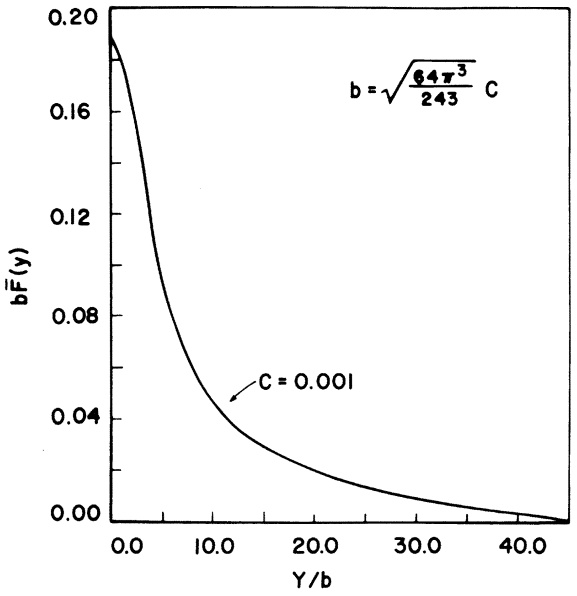

FIG. 8. $\bar{F}(y)$ for $c = 0.001$ scaled to be valid for all low concentrations.

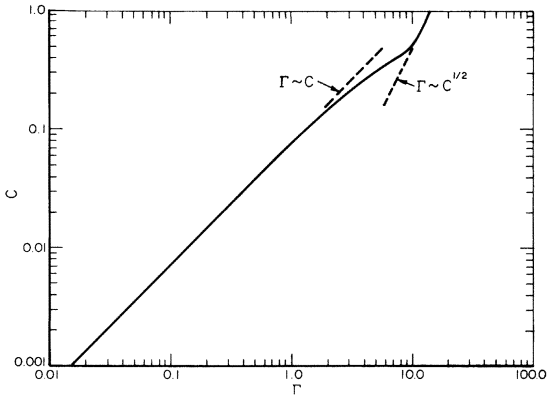

FIG. 9. Linewidth Γ vs c.

independent of the solutions to the local equations. This is a reflection of the fact that $[H_d, S_z] = 0$, where H_d is the truncated dipolar Hamiltonian. Thus our theory predicts that all but the zeroth moment of $\bar{\mathfrak{F}}_0(\omega)$ is zero, a fact which is in agreement with a Van Vleck moment analysis and with other theories. In the Sung-Arnold[9] theory, on the other hand, no such moment preservation occurs for the $\langle S_z S_z \rangle$ correlation function. Therefore although it is necessary in our theory to solve the local equations for both $\bar{g}_0(\omega)$ and $\bar{g}_1(\omega)$, the only nonlocal function that must be computed is $\bar{\mathfrak{F}}_1(\omega)$. This has been done for a variety of c ranging from 10^{-3} to 1; the results are summarized in Figs. 5–8. In those figures, the functions have been scaled to the dimensionless variables

$$y = \omega / [\tfrac{1}{12} s(s+1)]^{1/2} \omega_d , \tag{44}$$

$$\bar{F}(y) = \bar{\mathfrak{F}}_1(\omega) [\tfrac{1}{12} s(s+1)]^{1/2} \omega_d . \tag{45}$$

As can be seen from Figs. 5–8, the width of the line shape dramatically decreases with decreasing c, while the amplitude increases correspondingly. In fact, if one defines a linewidth as

$$\Gamma \equiv 1/\bar{F}(0), \tag{46}$$

then we find that Γ is proportional to $c^{1/2}$ for $0.5 \lesssim c \leq 1.0$, while it is proportional to c for $c \lesssim 0.1$. Both the large-[1-3,8] and[4,5,22] small-c behavior of the linewidth are in agreement with phenomenological and semiphenomenological theories. Furthermore, the small-c behavior is in agreement with the data of Grant and Strandberg[4,5] for EPR on low concentrations of the CR^{+3} ion in ruby. The predicted behavior of the linewidth as a function of concentration is summarized in Fig. 9.

It is clear from Figs. 5–8 that not only does the linewidth predicted by our theory change rapidly as a function of c, but so does the predicted line shape. As Fig. 5 shows, for large c the theoretical line shape shows a dip as y goes to zero. The limit of $c = 1$ is the only large-c case for which experimental data are available. In this limit frequency line-shape data exist for the ^{19}FNMR in CaF_2.[23] The predicted line shape and the experimental line shape are in considerable disagreement near $\omega = 0$. In particular, the experimental curve is somewhat flat on top before tailing off toward zero and does not display the dip produced by our theory. Detailed theoretical-experimental comparison for this case will be deferred to Sec. III C. However, it is worthwhile stating now that we believe the reason for this discrepancy lies in the intrinsic limitation of the bubble approximation itself. In particular, the bubble approximation gives the correct second moment for the line shape but does not preserve the fourth and higher moments. Because these higher moments, particularly the fourth, are not preserved, the line shape will not have the correct behavior except at times near zero. The only method we see for removing this discrepancy is to include higher-order diagrams in the diagrammatic expansion of the self-energy. One of us (P.A.F.) is currently pursuing this problem.

As can be seen from Figs. 6 and 7, as c decreases the dip in the line shape gradually flattens out into a shoulder, beginning at about $c = 0.3$, and finally disappears altogether at about $c = 0.01$. At the same time, the center of the line rises

and becomes increasingly Lorentzian in shape. We would like to emphasize that although we believe this general trend is correct the positions and amplitudes of the shoulders and tails of the line shapes depend on the details of $p(f;c)$ and, owing to numerical limitations, to some extent on the actual grid in f space that we chose in order to solve the integrals over that function. For economic as well as practical reasons, we had to limit the number of f points used in these integrations. We have found that varying this f grid does not affect the shape of the line at the center, but it can affect the positions and amplitudes of the shoulders and the amplitudes of the tails by a few percent for reasonable f grids. For a given c, however, if a shoulder is present for one such choice of the points in f space, it was found to be there regardless of how we varied the f grid. We believe then that the variations just mentioned are due to numerical uncertainties caused by practical limitations in going the f integrals and are *not* the result of defects in the basic theory itself. A more detailed discussion of $p(f;c)$ may be found in the Appendix.

As can be seen from Figs. 7 and 8, at extremely small c the line shape becomes more Lorentzian. This is in agreement with the observed EPR lineshape for small concentrations of Cr^{+3} ions in ruby[4,5] and is also in agreement with phenomenological and semiphenomenological theories.[4,5,22] The reason that we obtain agreement with experiment for the line shapes at small c and are in disagreement at $c=1$ is probably that at small c the higher moments do not contribute to the central peak, so the fact that the theory does not preserve them does not matter.

In the small-c region, the line shape scales with c. The line shapes at $c=0.001$ obtained from the numerically evaluated $p(f;c)$ and from the analytic form of $p(f;c)$, which is exact as $c\to 0$, are virtually identical, as expected. The line shape at this low concentration, shown in Fig. 8, looks rather Lorentzian over most of the region of appreciable spectral weight. However, the tail of the actual line shape falls off slower than the tail of a true Lorentzian until far out in the wings.

To summarize this subsection, the theory outlined above, although imperfect, has yielded the first *first-principles* prediction of the magnetic-resonance line shape in the dipolar lattice for the entire range of spin concentration c, and is the first to obtain the c dependence of both line shapes and linewidths at all concentrations. The linewidths predicted by this theory have a c dependence, which is in agreement with previous theories in both the high- and low-c limits[1-10] and is in agreement with experiment at small c.[4,5] Finally, the line shapes obtained at small c are also in agreement with experiment,[4,5] while the large-c line shapes show considerable deviation from experiment. The line shape at $c=1$ is discussed in detail in Sec. III C.

C. Results for $c=1$; comparison with experimental free induction decay for CaF_2

Since the case of $c=1$ is of particular experimental interest,[17] we feel that it deserves special attention. The most common experiments done in this case are measurements of the free induction decay of ^{19}F in CaF_2.[17] Thus, in order to quantitatively compare our $c=1$ results with the latest experimental data,[17] we have Fourier transformed the $c=1$ line shape shown in Fig. 5 to obtain the free induction decay (FID) for the dipolar lattice. Our results are shown in Fig. 10 (solid curve) along with the data of Englesberg and Lowe (triangles). The data were taken at temperatures such that $77 \geq T \geq 4.2$ K and with the magnetic field in the [100] direction. In the figure, the dimensionless time $\tau = \omega_d t$ has been used.

We believe that this theoretical FID curve represents the first published[24] entirely first-principles calculation of the FID function for the dipolar lattice. Blume and co-workers[25] have obtained similar results, but have not published them. Others[26,27] have obtained FID curves which are in better agreement with experiment than

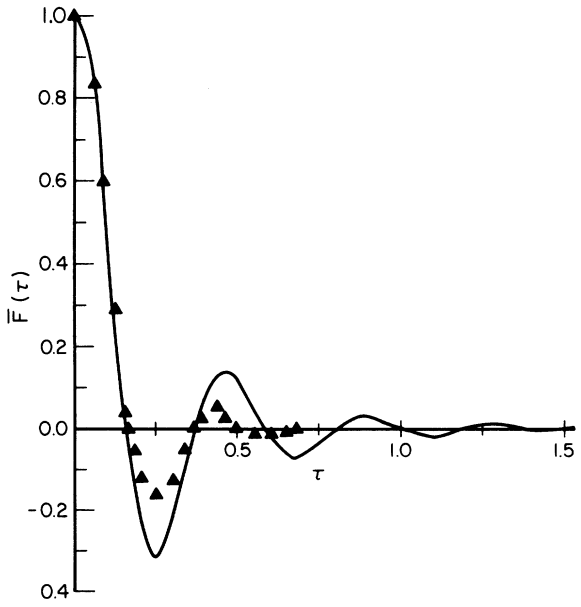

FIG. 10. Free induction decay $\bar{F}(\tau)$ for the dipolar lattice. Solid curve is the present theory and the triangles are the data of Englesberg and Lowe (Ref. 17).

ours, but they have used phenomenological[27] and semiphenomenological[26] theories. Our function, however, was obtained self-consistently using a theory which contains *no* line-shape assumptions or adjustable parameters. As is evident from Fig. 10 the best agreement at short times, before the first zero of the FID function. The discrepancy between theory and experiment[17] with regard to the positions of the zeros ranges from 5.65% for the first zero to 22.6% for the eighth zero. On the other hand, the amplitudes of oscillation are clearly not in good agreement with experiment; the theory and experiment differ by factors of 1.75 and greater for peaks beyond the initial one.

Again, we believe that the discrepancy is due to the limitations of the bubble approximation itself. In particular, the discrepancy in peak amplitudes is a reflection of the dip the frequency line shape has as y goes to zero. As discussed in Sec. III B, we believe that the dip, and thus the too-large oscillations in the FID, are caused by the nonconservation of the fourth and higher moments by the bubble approximation. We feel further, and phenomenological considerations indicate,[25] that including higher-order diagrams in the self-energy diagrammatic expansion will correct the discrepancy. One of us (P.A.F.) is currently pursuing this problem.

IV. SUMMARY AND CONCLUSIONS

We have developed a general, first-principles method for the calculation of dynamical spin correlation functions in a system of randomly distributed, strongly interacting spins with multipolar interactions. The method is valid in the high-temperature limit and is applicable at all spin concentrations c. As a numerical example, we have treated the case of dipolar forces and have calculated the magnetic-resonance frequency line shape for a variety of different values of c.

Although the theory does have its weaknesses, the general trend of the change in line shape and linewidth with c for the truncated dipolar interaction is correct, with the theoretical linewidth having the correct c dependence in both limiting cases ($c \to 1$ and $c \to 0$). The line shapes are also in agreement with experiment at small c.

Although the theory is applicable for any interaction which may be written in the form of Eq. (2), the only case which has been considered quantitatively thus far is the truncated dipolar case. From a qualitative analysis of the general tensor $\times r^{-n}$ interaction, however,[28] it is apparent that this formalism will give, at the very least, reasonable results for the c dependence of the linewidth in the general case. In particular, such an analysis shows that in the limit $c \to 1$, the theory predicts that $\Gamma \sim c^{1/2}\Gamma \sim c^{n/3}$. This is in agreement with the phenomenological theory of Hama *et al.*,[8] and is also in agreement with experiment[29,30] and previous theories[6-8,11,13] for quadrupolar systems ($n = 5$).

The quadrupolar case is especially relevant for the study of magnetic resonance in solid H_2.[6,7,11,13] In fact, this system was the original motivation for the development of the general formalism presented in Sec. II. Unfortunately, the formalism for this system is so much more complicated than the (already complicated) formalism for the dipolar system that at the present time it is not economically feasible to carry out the computer work necessary to solve this problem. In fact, the computational complexity of the formalism is perhaps its greatest practical limitation. We believe, however, that this is an unfortunate but necessary consequence of the physical complexity of the problem.

ACKNOWLEDGMENTS

The authors would like to thank Professor H. Ehrenreich, Professor L. P. Kadanoff, Professor D. Esterling, Professor D. Stroud, Professor T. Lubensky, and Professor R. A. Tahir-Kheli for helpful comments and criticisms. We also thank the Battelle Memorial Institute for the use of the CDC 6400 computer on which the numerical calculations were done.

APPENDIX: PROBABILITY DISTRIBUTION FUNCTION $p(f; c)$

The probability density $p(f; c)$ for the squared interaction strength f at concentration c is found under the assumptions of an infinite crystal and a random distribution of the spins, so that the probabilities of having the various lattice sites occupied by an impurity are independent of each other. Then the probability of any given site being occupied by a spin is just c and, for the case of one function $f(i)$ as in Eqs. (13), it can be shown that[31]

$$p(f; c) = \int_{-\infty}^{\infty} \frac{d\mu}{2\pi} e^{i\mu f} \prod_j{}' (1 - c + c e^{-i\mu g_{ij}}), \quad \text{(A1)}$$

where the product is over all lattice sites $j \neq i$ and, given the truncated dipolar interaction,

$$g_{ij} = (1 - 3\cos^2\Theta_{ij})^2 (a/|\vec{r}_{ij}|)^6; \quad \text{(A2)}$$

Θ_{ij} is the angle between the applied magnetic field and $\vec{r}_{ij} \equiv \vec{r}_i - \vec{r}_j$.

In general, $p(f; c)$ must be evaluated numerically. However, for $1 - c \ll 1$ and $c \ll 1$, it is possi-

ble to find approximate analytic expressions which are exact in the appropriate limit in each case. For $1-c \ll 1$, the distribution function may be approximated by

$$p(f;c) = [\pi(1-c)f_2]^{-1/2} \exp[-(f-cf_1)^2/(1-c)f_2], \tag{A3}$$

where $f_1 = \sum_j' g_{ij}$ and $f_2 = \sum_j' g_{ij}^2$. Note that for $c \to 1$ this Gaussian becomes a δ function, $p(f;1) = \delta(f-f_1)$, which is exactly correct. For $c \ll 1$, on the other hand, one can show that $p(f;c)$ is well approximated by[31]

$$p(f;c) = b(\pi f^3)^{-1/2} e^{-b^2/f}, \tag{A4}$$

where $b = (\frac{64}{243}\pi^3 c^2)^{1/2}$.

Thus we find that $p(f;c)$ is a function exhibiting a single, simple peak at both high and low c; for $c \approx 1$, the peak is located at a large value of $f = cf_1$, while for small c the maximum value of $p(f;c)$ occurs at $f = \frac{2}{3}b^2 = \frac{128}{729}\pi^3 c^2$ and goes to zero as c^2 does.

At intermediate c the behavior of $p(f;c)$ is much more complicated. From Eq. (A1) we see that it is actually a sum over an infinite number of δ functions whose arguments have zeros distributed between $f=0$ and $f=f_1$. We have determined this distribution by computing the weights and arguments of the δ functions arising from as many as 300 lattice shells surrounding the point $\vec{r}_i$. As c decreases from unity, more and more shells must be included in the sum to obtain good convergence; the maximum number of 300 was required at the minimum value of c for which results are presented here, specifically, at $c=0.001$.

For purposes of integrating $p(f;c)$ over f, we have converted the sum of δ functions to a less singular function by dividing f space into many small segments, each of width Δf. Then the weights of all of the δ functions having zero argument in a given increment Δf are summed and the sum is divided by Δf. The result becomes the value of $p(f;c)$ at the center of the interval in question. By taking Δf sufficiently small ($\Delta f = 10^{-7}$ for $c=0.001$ and $\Delta f = 0.005$ for $c \approx 1$) on the scale of variations of the envelope of $p(f;c)$, we guarantee that this smoothing has a negligible effect on any of the calculated correlation functions.

Some representative results for $p(f;c)$ are shown in Figs. 1–4. Starting at $c=1$, this function is just $\delta(f-f_1)$. As c decreases, the peak broadens into a Gaussian centered at cf_1. This is a reasonable description of $p(f;c)$ for $c \gtrsim 0.95$, although some structure begins to appear in the peak even at larger values of c and, also, additional peaks start to emerge at smaller f. By $c=0.8$, these peaks are well established, as shown in Fig. 1 (solid line). Note that the peaks at larger values of f tend to be larger in magnitude than those at smaller f, although there is not a monotonic increase of peak height with f even at this rather large concentration.

As c decreases further, the peaks at small and intermediate f grow steadily in magnitude at the expense of those at large f; by the time c reaches 0.5, the distribution is completely altered in appearance, with the central peak at $f = \frac{1}{2}f_1$ being the largest and six peaks being symmetrically arranged on either side. The case of $c=0.5$ is shown in Fig. 1 (dashed line).

For $c < 0.5$, the distribution continues to shift to lower values of f; at $c=0.2$, for example, it is very nearly the mirror image of the distribution at $c=0.8$ reflected in f space through the point $f = \frac{1}{2}f_1$. In Fig. 2 we show the first two peaks that remain at $c=0.1$; the other peaks have become quite small by this concentration. Note in this figure that structure is beginning to appear in each peak. This effect increases with decreasing c as may be seen in Fig. 3, where a part of the first peak at $c=0.02$ is shown; peaks beyond the first are quite negligible at this and smaller concentrations. Finally, at very small c, the structure dies away and the computed $p(f;c)$ becomes smooth, approaching the analytic result, Eq. (A4), which is expected to be valid for $c \ll 1$. In Fig. 4 we see that these two functions are already quite close to each other at $c=0.001$, although there is still some structure present in the computed function, causing it to fluctuate a bit around the analytic distribution. At this particular concentration we have computed the correlation functions using both distribution functions shown in Fig. 4; as is shown in Fig. 8, the two sets of results are the same for all practical purposes, and thus imply that there is no need to evaluate $p(f;c)$ numerically for $c < 0.001$.

---

*Present address: Laboratoire de Physique Expérimentale, Département de Physique, École Polytechnique Fédérale de Lausanne, 33 Av. de Cour, CH-1007 Lausanne, Switzerland.

†Supported in part by the NSF.

[1]H. Margenau, Rev. Mod. Phys. 8, 22 (1935).

[2]P. W. Anderson, Phys. Rev. 82, 842 (1951).

[3]C. Kittel and E. Abrahams, Phys. Rev. 90, 238 (1953).

[4]W. J. C. Grant and M. W. Strandberg, Phys. Rev. 135, A715 (1964).

[5]W. J. C. Grant and M. W. Strandberg, Phys. Rev. 135, A727 (1964).

[6]C. C. Sung, Phys. Rev. 167, 271 (1968).
[7]A. B. Harris, Phys. Rev. B 2, 3495 (1970).
[8]J. Hama, T. Inuzuka, and T. Nakamura, Prog. Theor. Phys. 48, 1769 (1972).
[9]C. C. Sung and L. G. Arnold, Phys. Rev. B 7, 2095 (1973).
[10]C. Ebner and C. C. Sung, Phys. Rev. B 8, 5226 (1973).
[11]C. Ebner and C. W. Myles, Phys. Rev. B 12, 1638 (1975).
[12]C. W. Myles and P. A. Fedders, Phys. Rev. B 9, 4872 (1974).
[13]C. W. Myles and C. Ebner, Phys. Rev. B 11, 2339 (1975); 12, 1608(E) (1975).
[14]C. W. Myles, Phys. Rev. B 11, 3225 (1975).
[15]C. W. Myles, Phys. Rev. B 11, 3238 (1975).
[16]P. A. Fedders, C. W. Myles, and C. Ebner, AIP Conf. Proc. 24, 338 (1975).
[17]See, for example, M. Englesberg and I. J. Lowe, Phys. Rev. B 10, 822 (1974).
[18]G. F. Reiter, Phys. Rev. B 5, 222 (1972).
[19]B. Velický, S. Kirkpatrick, and H. Ehrenreich, Phys. Rev. 175, 747 (1969).
[20]See, for example, C. P. Slichter, *Principles of Magnetic Resonance* (Harper and Row, New York, 1963).
[21]C. W. Myles, Ph.D. thesis (Washington University, 1973) (unpublished).
[22]A. Abragam, *The Principles of Nuclear Magnetism* (Oxford U. P., London, 1970), p. 120.
[23]Reference 22, p. 116.
[24]This figure was also presented in Ref. 16.
[25]M. Blume (private communication).
[26]F. C. Barreto and G. F. Reiter, Phys. Rev. B 6, 2555 (1972).
[27]G. W. Parker and F. Lado, Phys. Rev. B 9, 22 (1974).
[28]P. A. Fedders (unpublished).
[29]L. I. Amstutz, H. Meyer, S. M. Meyers, and R. L. Mills, J. Phys. Chem. Solids 30, 2693 (1969).
[30]F. Weinhaus and H. Meyer, Phys. Rev. B 7, 2974 (1973).
[31]P. A. Fedders, Phys. Rev. B 11, 1020 (1975).